Chemical order in 1/1 Al(Si)-Cu-Fe approximant phases

V. Simonet,[1,*] F. Hippert,[2] R. A. Brand,[3] Y. Calvayrac,[4] J. Rodriguez-Carvajal,[5] and A. Sadoc[6]
[1]*Laboratoire Louis Néel, CNRS, B.P. 166, F-38042 Grenoble Cedex 9, France*
[2]*Laboratoire des Matériaux et du Génie Physique, ENSPG, B.P. 46, F-38402 Saint Martin d'Hères Cedex, France*
[3]*Institute of Physics, Universität Duisburg-Essen, D-47048 Duisburg, Germany*
[4]*CECM/CNRS, 15 Rue G. Urbain, F-94407 Vitry Cedex, France*
[5]*Laboratoire Léon Brillouin (CEA-CNRS), CEA/Saclay, F-91191 Gif sur Yvette Cedex, France*
[6]*Laboratoire de Physique des Matériaux et des Surfaces, Université de Cergy-Pontoise, F-95031 Neuville sur Oise Cedex, France*
(Received 20 October 2004; revised manuscript received 4 February 2005; published 28 July 2005)

The structures of the cubic α'-$Al_{71.7}Si_7Cu_{3.8}Fe_{17.5}$ and α-$Al_{55}Si_7Cu_{25.5}Fe_{12.5}$ phases, 1/1 approximants of Al-Cu-Fe quasicrystals, are revisited. The chemical order in the α phase is inferred from joined x-ray and neutron powder diffraction data refinements and from extended x-ray absorption fine structure (EXAFS) studies at both Fe and Cu *K*-edges. The existence of crystallographic sites randomly occupied by both Al and Cu atoms, or by a combination of Al, Cu, and Fe atoms, allows the understanding of the chemical substitution mechanisms defining the existence domain of this approximant.

DOI: 10.1103/PhysRevB.72.024214 PACS number(s): 61.44.Br, 61.10.Ht, 61.10.Nz, 61.12.Ld

I. INTRODUCTION

Thermodynamically stable quasicrystals (QCs) exist in many different ternary systems such as Al-Pd-Mn, Al-Cu-Fe, Al-Cu-Ru, and Al-Pd-Re.[1] They are characterized by the presence of long-range order but an absence of translational periodicity. They present physical properties unexpected for alloys made of metallic elements, such as a reduced density of states (DOS) at the Fermi level and a large resistivity which increases with decreasing temperature.[2,3] Their atomic structure can be generated by the "cut and projection" method[4,5] where the real three-dimensional (3D) space is generated by an irrational cut of a 6D periodic lattice with a slope equal to the golden mean $\tau=(1+\sqrt{5})/2$. If a good description of the atomic positions is thus obtained, their occupation by the different chemical species is still not completely solved.[6,7] This is an important question because the chemical local order and especially the Al-transition metal bonds play a central role in determining the atypical electronic properties of QCs and probably their stability through the pseudogap formation.[8] Another way to clarify this question is provided by the existence of approximants. These are crystalline phases obtained by a rational cut of the 6D space, with a slope equal to a rational approximant p/q of τ. With increasing integers p and q, i.e., with increasing approximant order, the size of the unit cell increases and the local structure approaches that of the parent quasicrystalline phase on an increasing scale. The QC structure is often described as a packing of clusters with icosahedral symmetry as the Mackay[9] or Bergman[10] clusters. Such clusters are found even in the lowest order approximants ($p/q=1/1$), which are cubic phases with a cell parameter a close to 12.5 Å. Approximants of various orders have been identified in most systems where QCs exist. Their electronic properties are found close to those of QCs.[11,12] Therefore the determination of the atomic structure of approximants is an important task. First, it should help to understand the chemical local order in QCs. Second, it allows one to investigate the interplay between structural and electronic properties, especially through band structure calculations.[11,13,14]

The Al-Cu-Fe system is especially interesting because several approximants, with various orders, have been identified.[15,16] At 700 °C, a face-centered (*F*-type) icosahedral QC exists within a small triangular concentration domain centered around the composition $Al_{62}Cu_{25.5}Fe_{12.5}$. At lower temperature this domain reduces to a narrow line segment. High order approximants, either pentagonal ($p/q=4/3$), rhombohedral ($p/q=3/2$) or orthorhombic (with $p/q=3/2$, 11/7 or 2/1 depending on the spatial direction) are found at 700 °C along a nearby parallel line, centered at the composition $Al_{62.8}Cu_{26}Fe_{11.2}$. The same well defined substitution law is obeyed along both lines: 1 Cu being replaced by 0.6 Al+0.4 Fe. For each of these stability lines, the average number of conduction electrons per atom, e/a, corresponds to a constant, revealing a close relationship between electronic and structural properties. The electronic properties of these high order approximants are quite similar to those of QCs (Refs. 12, 17, and 18) but unfortunately, up to now, their structure could not be determined because of its complexity and of the absence of single crystals. A particularity of the Al-Cu-Fe system is that substitution of a few percent of Si for Al leads to the formation of two cubic 1/1 approximants with different compositions.[11,16,19] One of them exists for Cu and Fe contents similar to those in the parent icosahedral QC phase and its electronic properties are found similar to those of QCs.[19] It will be denoted α hereafter, following the notations of Refs. 16 and 19. The elongated shape of its existence domain for 650 °C at a constant Si composition of 7 at % (Fig. 1) corresponds to the same substitution law as in QCs and high order approximants.[16,20] The second cubic 1/1 phase exists only for a fixed Fe composition (17.4 at %) and a small amount of Cu (around 4 at %) and Si (around 7 at %).[16] Although this second phase has often been noted α in the literature, here we label it α', in order to distinguish it from the first one. The occupied crystallographic positions in the α and α' phases are almost identical.[21–24] It is then striking to find them in distinct composition domains in the Al(Si)-Cu-Fe phase diagram. The aim of the present work, is

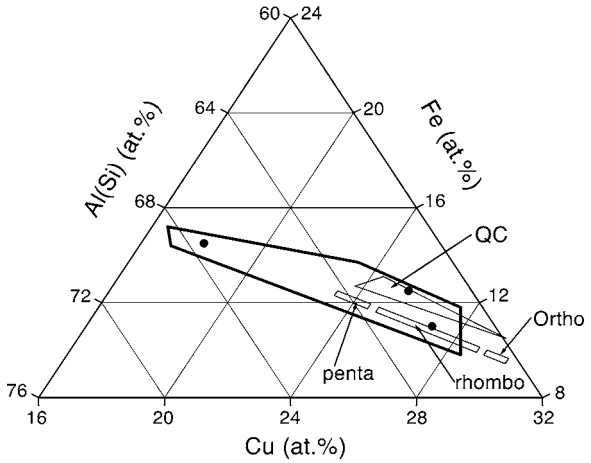

FIG. 1. Composition domain at 650 °C of the 1/1 α-Al(Si)-Cu-Fe approximant (thick lines) (Refs. 16 and 20), for a constant Si composition of 7 at %. The existence domains at 700 °C of the Al-Cu-Fe icosahedral quasicrystal (QC) and of its high order approximants (pentagonal, rhombohedral, and orthorhombic) are also shown as thin lines (from Ref. 15). The compositions of the three studied α samples are indicated by dots.

to determine their chemical decoration and to understand the substitution mechanisms underlying the existence domain of the α phase and hence its stability.

We combined neutron and x-ray powder diffraction and extended x-ray absorption fine structure (EXAFS) at the Cu and Fe *K*-edges. Indeed, EXAFS data turned out to be necessary to distinguish between different models compatible with the diffraction data. Before presenting results in Sec. IV, the state of the art about the structural models of the α' and α-Al(Si)-Cu-Fe phases is first recalled in Sec. II. This will make clear why further investigations of their structure were indeed necessary. Samples and experiments are briefly described in Sec. III. Finally, in Sec. V the obtained structures for the α' and α are compared to those of 1/1 approximants in other systems with a particular emphasis on the position of the transition metal atoms.

II. STRUCTURAL MODELS OF 1/1 Al(Si)-Cu-Fe APPROXIMANTS: STATE OF THE ART

The atomic structure of the α'-Al(Si)-Cu-Fe phase[21,22] is almost isomorphous to that of the cubic $Al(Si)_{82.6}Mn_{17.4}$ phase (with about 10 at % Si),[25,26] which is a 1/1 approximant of the Al(Si)-Mn QC.[27,28] These two cubic phases have 138 atoms per unit cell and their cubic cell parameter a is close to 12.6 Å. When comparing them, the Fe atoms correspond to the Mn ones. However, an $Al(Si)_{82.6}Fe_{17.4}$ phase does not exist. The introduction of a few percent of Cu,[16,22] or the substitution of about 20% of Fe by Mn,[11,21] is found necessary to stabilize the structure. The nature of the crystallographic sites occupied by the Cu atoms is an open question. Strictly speaking, the primitive Al(Si)-Mn phase (space group $Pm\bar{3}$) should not be considered as isomorphous to the body-centered α'-Al(Si)-Cu-Fe phase (space group $Im\bar{3}$). However, this symmetry change results from minor modifications in the repartition of the so-called glue atoms [sites labeled (10), (11), and (12) in Table I and Fig. 2], all the other atomic positions being identical in the two phases.[11] This difference will be neglected in the following.[29]

The existence of the α-Al(Si)-Cu-Fe phase has been reported more recently.[19] Its structure has been investigated by two groups for the same nominal composition $Al_{55}Si_7C_{25.5}Fe_{12.5}$. Takeuchi *et al.* have analyzed powder x-ray diffraction data, using the 1/1 Al(Si)-Mn atomic structure as a starting point.[23] Puyraimond *et al.* have refined single crystal x-ray diffraction data, starting from a theoretical model resulting from a perpendicular shear applied to the parent QC model.[24] The two models, denoted hereafter *T* and *P*, lead to the same atomic structure (space group $Pm\bar{3}$) with 136.4 atoms per unit cell and $a=12.321$ Å for model *T* and 137.7 atoms per unit cell and $a=12.312$ Å for model *P*. The refined compositions are $Al_{57.3}Si_{7.1}Cu_{23.85}Fe_{11.75}$ for model *T* and $Al(Si)_{61.9}Cu_{26.8}Fe_{11.3}$ for model *P*. The occupied atomic positions are exactly the same in the two models and very close to those in the 1/1 Al(Si)-Mn and α'-Al(Si)-Cu-Fe phases. However, models *T* and *P* lead to significantly different chemical orders, as described hereafter.

The atomic structure of the 1/1 Al(Si)-Mn, α' and α-Al(Si)-Cu-Fe approximants can be described in terms of clusters with icosahedral symmetry made of concentric shells with increasing size (Fig. 2). The same atomic structure, and hence the same clusters, are also encountered in 1/1 approximants in the Al(Si)-Re,[30] Al-Cu-Ru,[31] and Al(Si)-Cu-Ru (Ref. 32) systems (see Sec. V). One can first identify two Mackay clusters, with no common atom, one centered at (0, 0, 0) and the other one at (1/2, 1/2, 1/2). A Mackay cluster contains 54 atoms if its center is empty.[9] It consists of an inner icosahedron (radius ~2.4 Å) surrounded by a larger icosidodecahedron and another icosahedron, both with radii close to 4.7 Å. The cluster description of the structure can be extended by including the remaining atoms, usually called glue atoms in the literature. These atoms can indeed be arbitrarily attached to one or the other Mackay cluster. Following the presentation of Sugiyama *et al.* in Ref. 26, two additional shells are added to the Mackay cluster located at (0, 0, 0) in Fig. 2. The first one contains 60 atoms forming a rhombicosidodecahedron (radius ~6.4 Å). The second one is an icosahedron (radius ~7.3 Å). Note that the same atoms [from crystallographic site (7) following the notations of Tables I and II] are used to build the rhombicosidodecahedron centered at (0, 0, 0) and the icosidodecahedron of the Mackay cluster centered at (1/2, 1/2, 1/2). Therefore, for radius larger than 4.7 Å, a cluster description implies interpenetrating clusters. The centers of the two Mackay clusters are empty in the 1/1 Al(Si)-Mn and α'-Al(Si)-Cu-Fe phases but the (0, 0, 0) position is occupied in α-Al(Si)-Cu-Fe. The presence of this central atom has strong consequences on the geometry of the first shell of the Mackay cluster which loses its icosahedral character.[23]

The chemical decoration of these clusters is given in Table I. The Si atoms have been treated as Al ones in all cases. The α' phase considered in the second column of Table I is an hypothetical $Al(Si)_{82.6}Fe_{17.4}$ phase, without Cu, analyzed here as if it was primitive.[29] It is isomorphous to

TABLE I. Chemical decoration of the icosahedral clusters in several 1/1 approximants. Shell labels "ico," "icosi," and "rhombico" stand for icosahedron, icosidodecahedron, and rhombicosidodecahedron, respectively (see Fig. 2). The crystallographic sites are numbered as in Table III. The nature and number of the atoms on each site are reported. The Si and Al atoms are not distinguished and are all labeled Al. The α' phase is an hypothetical $Al(Si)_{82.6}Fe_{17.4}$ phase. Four models are given for the α_1-$Al_{55}Si_7Cu_{25.5}Fe_{12.5}$ phase: previously published models (*P* and *T*), model *A* obtained from the present powder x-ray and neutron diffraction data (Sec. IV B 1 and Table III) and the final model B obtained from the EXAFS analysis (Sec. IV B 2). Models for the α_2-$Al_{60.5}Si_7Cu_{18}Fe_{14.5}$ and α_3-$Al_{57}Si_5Cu_{27}Fe_{11}$ phases are deduced from the EXAFS analysis only (Sec. IV B 3). The composition of the 1/1 Al-Cu-Ru approximant is $Al_{57.2}Cu_{31.4}Ru_{11.4}$.

Shell	Site	Al(Si)-Mn	α'	Al(Si)-Cu-Fe α_1 Model *P*	α_1 Model *T*	α_1 Model *A*	α_1 Model *B*	α_2	α_3	Al-Cu-Ru
		Ref. 26	Ref. 21	Ref. 24	Ref. 23					Ref. 31
					Cluster at (0, 0, 0)					
center	(1)	empty	empty	Fe	Cu	Fe	Fe	Fe	Fe	Ru
	1a			1	0.91	1	1	1	1	1
ico	(2)	Al	Al	Al	Al	Al	Al	Al	Al	Al
	12j	12	12	10.7	9.5	10.1	10.1	10.1	10.1	2.16
icosi	(3)	Al	Al	Cu/Al	Cu/Al	Cu/Al	Cu/Al	Cu/Al	Cu/Al	Cu/Al
	241	24	24	17.1/6.9	16.8/7.2	16.8/7.2	15.2/8.8	11.2/12.8	14.95/9.05	17.3/6.7
	(4)	Al	Al	Cu/Al	Cu/Al	Cu/Al	Cu	Cu/Al	Cu	Cu/Al
	6e	6	6	4.25/1.75	4.2/1.8	3.8/2.2	6	5.5/0.5	6	5.45/0.55
ico	(5)	Mn	Fe	Fe	Cu/Al	Cu/Al/Fe	Cu/Al/Fe	Cu/Al/Fe	Cu/Al/Fe	Cu/Al
	12j	12	12	12	8.65/3.35	5.6/2.4/4	5.15/2.85/4	0.1/5.2/6.7	7.4/2.6/2	10.0/2.0
rhombico	(11)	Al	Al	Al/Fe	Al	Al	Al	Al	Al	Al
	12j	12	12	11.6/0.4	12	12	12	12	12	12
	(12)	Al	Al	Al/Fe	Al	Al	Al	Al	Al	Al
	12k	12	12	11.6/0.4	12	12	12	12	12	12
ico	(10)	Al	Al	Cu	Cu/Fe	Cu/Al	Cu	Cu	Cu	Cu
	6f	6	6	6	2.0/4.0	5.6/0.4	6	6	6	6
					Cluster at (1/2,1/2,1/2)					
center	1b	empty	empty	empty	empty	empty	empty	empty	empty	Ru 1
ico	(6)	Al	Al	Al/Fe	Al	Al/Cu	Al/Cu	Al/Cu	Al/Cu	Al
	12k	12	12	10.3/1.7	12	9.2/2.8	9.85/2.15	10.45/1.55	9.8/2.2	11
icosi	(7)	Al	Al	Al	Al	Al	Al	Al	Al	Al
	241	24	24	24	24	24	24	24	24	24
	(8)	Al	Al	Al	Al	Al	Al	Al	Al	Al
	6h	6	6	6	6	6	6	6	6	6
ico	(9)	Mn	Fe	Cu/Al	Fe	Fe	Fe	Fe	Fe	Ru
	12k	12	12	9.6/2.4	12	12	12	12	12	12

the $Al(Si)_{82.6}Mn_{17.4}$ phase (first column of Table I). The Fe (or Mn) atoms occupy the outer icosahedron of each Mackay cluster, the remaining shells being filled with Al(Si) atoms. In the real α'-$Al_{71.7}Si_7Cu_{3.8}Fe_{17.5}$ phase studied here, it is reasonable to assume that the Cu atoms occupy partially some of the Al(Si) sites. For the α-$Al_{55}Si_7Cu_{25.5}Fe_{12.5}$ approximant, the results of models *P* and *T* are presented. Although both models lead to similar electronic densities and hence to a good agreement with x-ray diffraction patterns, they lead to significantly different chemical occupations on sites (1), (5), (6), (9), and (10). As a result, the predicted local environments around Fe and Cu atoms are different in

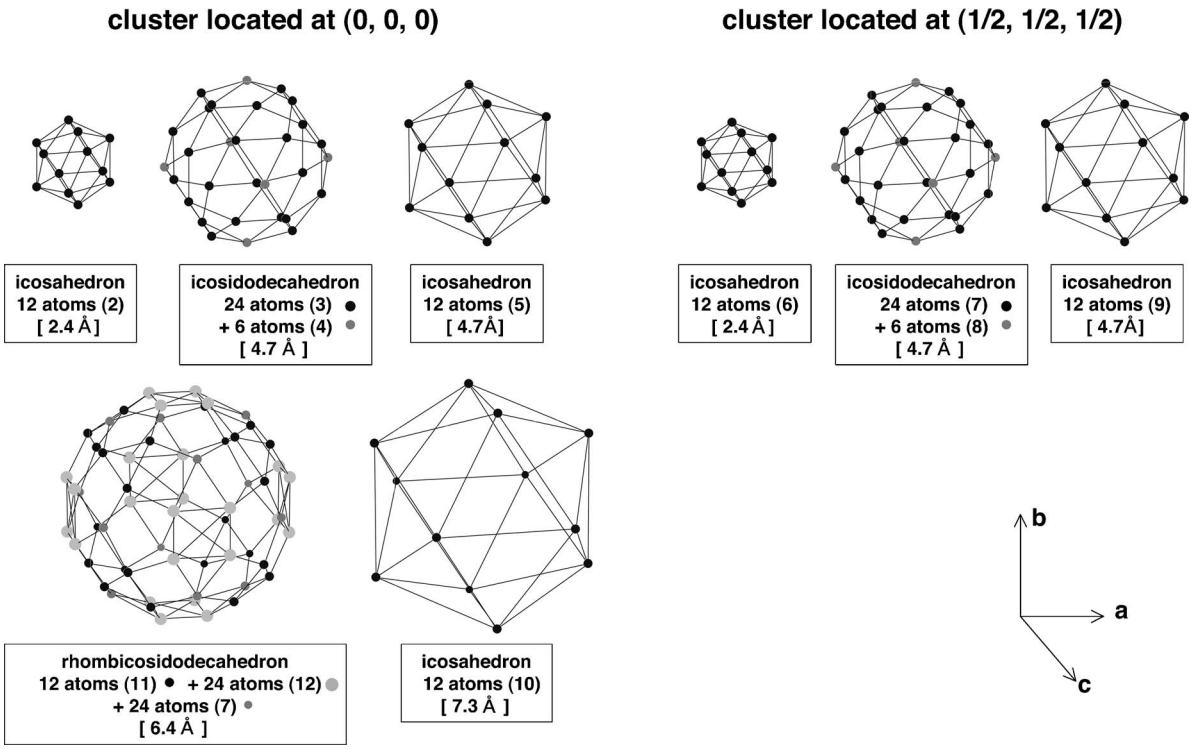

FIG. 2. Atomic structure of the clusters with icosahedral symmetry centered at (0, 0, 0) and (1/2, 1/2, 1/2) in 1/1 approximants in the Al(Si)-Cu-Fe system. For each cluster, the concentric shells with increasing size are shown separately. The crystallographic sites used to build each shell are indicated. Their labels (numbers within parentheses) follow the notations of Tables I and III. The average radius of the shell is indicated. In the α-Al(Si)-Cu-Fe approximant, an additional atom (not represented in the figure) occupies the (0, 0, 0) position and induces an important disorder in the first shell, which looses its icosahedral character. The chemical decoration of these clusters is given in Table I.

the two models. This contradiction points out that x-ray diffraction techniques alone are not sufficient to determine the chemical order in the α-Al(Si)-Cu-Fe phase, because of the lack of contrast between Cu and Fe atoms. In addition, these two models were found unable to explain the present EXAFS data at the Fe and Cu *K*-edges for the α-$Al_{55}Si_7Cu_{25.5}Fe_{12.5}$ phase. Therefore, we have undertaken a new structural determination of this phase by combining neutron and x-ray powder diffraction and EXAFS. The obtained chemical decorations, to be discussed hereafter, are presented in Table I, together with results for the two other α samples studied in the present work and results for the 1/1 Al-Cu-Ru approximant[31] (see Sec. V).

III. SAMPLES AND EXPERIMENTS

A. Samples

Three different α samples, of nominal composition $Al_{55}Si_7Cu_{25.5}Fe_{12.5}$ (α_1), $Al_{60.5}Si_7Cu_{18}Fe_{14.5}$ (α_2), and $Al_{57}Si_5Cu_{27}Fe_{11}$ (α_3), have been studied. The Fe and Cu compositions of α_1 and α_3 are the same as those of a stable QC and a rhombohedral approximant respectively (without Si). The Fe and Cu compositions of α_2 do not correspond to a single phase in the ternary Al-Cu-Fe phase diagram. These three samples span the existence domain of the α-Al(Si)-Cu-Fe phase at 650 °C (Fig. 1). The studied α' sample has the composition $Al_{71.7}Si_7Cu_{3.8}Fe_{17.5}$.

TABLE II. Structural parameters from the EXAFS fits of α'-$Al_{71.7}Si_7Cu_{3.8}Fe_{17.5}$ at the Fe *K*-edge at 15 K and of $Al_{72.5}Mn_{17.4}Si_{10.1}$ at the Mn *K*-edge at room temperature. The Si atoms are treated as Al atoms. The calculations have been performed by summing on all scattering paths but the results are presented here using a pseudoshell description, with *N* the total number of neighbors within a given pseudoshell and $\langle r \rangle$ their mean distance from the absorbing atom (Å). $\delta r/r$ is the relative variation of the distances with respect to those calculated from crystallographic data. σ^2 (Å^2) is the relative mean displacement for an individual scattering path. rf is the goodness of the fit. For α'-Al(Si)-Cu-Fe, two kinds of Al(Si) atoms were considered with a different σ^2 value (see text). The errors bars are of the order of 0.02 Å for the mean distances and of 0.002 Å^2 for the σ^2 values.

α'-Al(Si)-Cu-Fe	*K*-edge	rf	N_{Al}	$\langle r_{Al} \rangle$	$(\delta r/r)_{Al}$	σ^2_{Al}	N_{Al}	$\langle r_{Al} \rangle$	$(\delta r/r)_{Al}$	σ^2_{Al}	N_{Cu}	$\langle r_{Cu} \rangle$	$(\delta r/r)_{Cu}$	σ^2_{Cu}
	Fe	0.002	5.5	2.550	0.0011	0.0039	5.35	2.734	0.0041	0.0068	0.65	2.731	0.0031	0.0020
Al(Si)-Mn	*K*-edge	rf	N_{Al}	$\langle r_{Al} \rangle$	$(\delta r/r)_{Al}$	σ^2_{Al}								
	Mn	0.003	11.5	2.647	−0.0036	0.0089								

All samples were prepared at CECM from the pure elements by induction melting in an alumina crucible under a controlled pure helium atmosphere flow. The entire ingots were remelted by induction heating and rapidly quenched by planar flow casting on a rotating copper wheel, under pure helium atmosphere. The obtained ribbons have been then annealed under high vacuum: ~24 h at 650 °C for the α samples, 72 h at 600 °C for the α' sample.[16] The ribbons have been ground into a fine powder for the diffraction and EXAFS experiments. The single phase character of the four studied samples has been established by inspection of their x-ray diffraction patterns where no spurious Bragg reflection could be detected.

B. Powder diffraction

X-ray and neutron powder diffraction experiments were performed at room temperature on the α_1 sample. The powder x-ray diffraction data ($\lambda = 1.94$ Å) were collected using a rotating sample holder in the 2θ range [7°–120°]. The neutron powder diffraction experiment was performed at Laboratoire Léon Brillouin on the high resolution powder diffractometer G4.2. The diffractometer, situated in a guide of cold neutrons, is equipped with a focusing Ge monochromator and a bank of ten ^{3}He detectors having Soller collimators of 10′ divergence. The measurements were performed in the 2θ range [6°–130°] at a wavelength of 2.593 Å. Data from both experiments were analyzed using the Rietveld refinement procedure implemented in the FullProf code.[33]

C. EXAFS

X-ray absorption spectra were measured on the D42 beamline of the DCI storage ring at LURE (Laboratoire pour l'Utilisation du Rayonnement Electromagnétique, Orsay, France). The x-ray absorption coefficient μ was measured in transmission mode. The incident energy was varied by 0.2 eV steps using a channel cut Si(331) single crystal monochromator. Measurements were made at 15 K on the three α samples at the Cu (8979 eV) and Fe (7112 eV) K-edges and on the α' sample at the Fe K-edge only. The 1/1 $Al_{72.5}Mn_{17.4}Si_{10.1}$ approximant was studied at the Mn K-edge (6537 eV) at room temperature.

The energy dependence of μ at energies above the edge yields information on the local order around the absorbing atom (distances and nature of neighboring atoms). Data were analyzed by using the FEFF package.[34] The normalized EXAFS oscillations $\chi(k)$ were first extracted from the measured absorption coefficient $\mu(E)$ by removing the absorption background using the AUTOBK program, which minimizes the modulus of the Fourier transform of $\chi(k)$ at short distances r (lower than the smallest atomic bond). Here k is the photoelectron wave number given by $k = \sqrt{2m(E-E_0)/\hbar^2}$, where E is the photon energy, E_0 is the edge energy, and m is the electron mass. Next, the Fourier transform (denoted FT) of the k^2 weighted $\chi(k)$ function was calculated, using a Hanning window in the k-range [3.4–12 Å^{-1}]. Then, the EXAFS oscillations contributing to a restricted r-range have been isolated by an inverse Fourier-transform (denoted IFT) leading to a Fourier filtered $k^2\chi(k)$ function. The r-ranges for the IFT were [1.7–3 Å] at the Mn and Fe K-edges and [1.3–3.1 Å] at the Cu K-edge.

For an absorbing central atom surrounded by N identical atoms at a distance r, when considering only single scattering paths, EXAFS oscillations created by the backscattering of the photoelectron by the neighboring atoms are given by

$$\chi(k) = -S_0^2 \frac{N}{kr^2} F(k,\pi) e^{-2k^2\sigma^2} e^{-2r/\lambda(k)} \sin(2kr + 2\delta(k) + \Phi(k)). \quad (1)$$

σ^2 is the relative mean displacement [Debye-Waller (DW) factor], which takes into account both the dynamical disorder and a possible small structural disorder. S_0^2 is the amplitude reduction factor accounting for many-body effects within the absorbing central atom. It was fixed to 0.74 for the Fe (and Mn) K-edges and to 0.9 for the Cu K-edge from EXAFS studies of the simple ω-$Al_{70}Cu_{20}Fe_{10}$ phase.[35] The scattering amplitude $F(k,\pi)$ and phase shift $\Phi(k)$, which depend on the nature of the neighboring atom, the absorbing atom phase shift $\delta(k)$ and the photoelectron mean free path $\lambda(k)$ were calculated using the FEFF program.

The FT or IFT data were fitted with the FEFFIT program.[34] No distinction was made between Al and Si atoms, which have almost the same backscattering effect. As usual, an additional parameter, namely an energy shift ΔE_0, was introduced in order to account for different choices of the edge energy E_0 in the experimental data analysis and in the FEFF calculations.[36] Note that the FT data cannot be identified with a radial distribution, because of the k-dependent phase and amplitude terms in the $\chi(k)$ expression [Eq. (1)].

IV. RESULTS

A. α'-Al(Si)-Cu-Fe approximant

The experimental FT of $k^2\chi(k)$ and the Fourier filtered $k^2\chi(k)$, obtained by IFT as explained in Sec. III C, at 15 K at the Fe K-edge in the α'-$Al_{71.7}Si_7Cu_{3.8}Fe_{17.5}$ are shown in Fig. 3. They are compared to results for $Al_{72.5}Mn_{17.4}Si_{10.1}$ at room temperature at the Mn K-edge. For both samples, the FT corresponding to first neighbors around Fe or Mn atoms is constituted of one main peak, narrower and higher in amplitude for the α'-$Al_{71.7}Si_7Cu_{3.8}Fe_{17.5}$ sample due to the lower temperature of measurement. A small bump on the right-hand side of the main peak is more marked in the case of the α' sample. The filtered $k^2\chi(k)$ for both samples present a maximum at k values around 5 Å^{-1}, which is characteristic of Al(Si) neighbors. Indeed, the position of the maximum of the backscattering amplitude depends on the atomic weight of the neighboring atoms. It lies in the low k-region for light atoms (such as Al or Si) and at higher k values for heavier atoms (Cu, Fe, Mn). A noticeable difference between the filtered $k^2\chi(k)$ of both samples is the presence of a second amplitude maximum at higher k values (around 10 Å^{-1}) in the case of α'-$Al_{71.7}Si_7Cu_{3.8}Fe_{17.5}$, but not of $Al_{72.5}Mn_{17.4}Si_{10.1}$. This feature suggests the presence of heavier Cu neighbors, as confirmed by the fits discussed below.

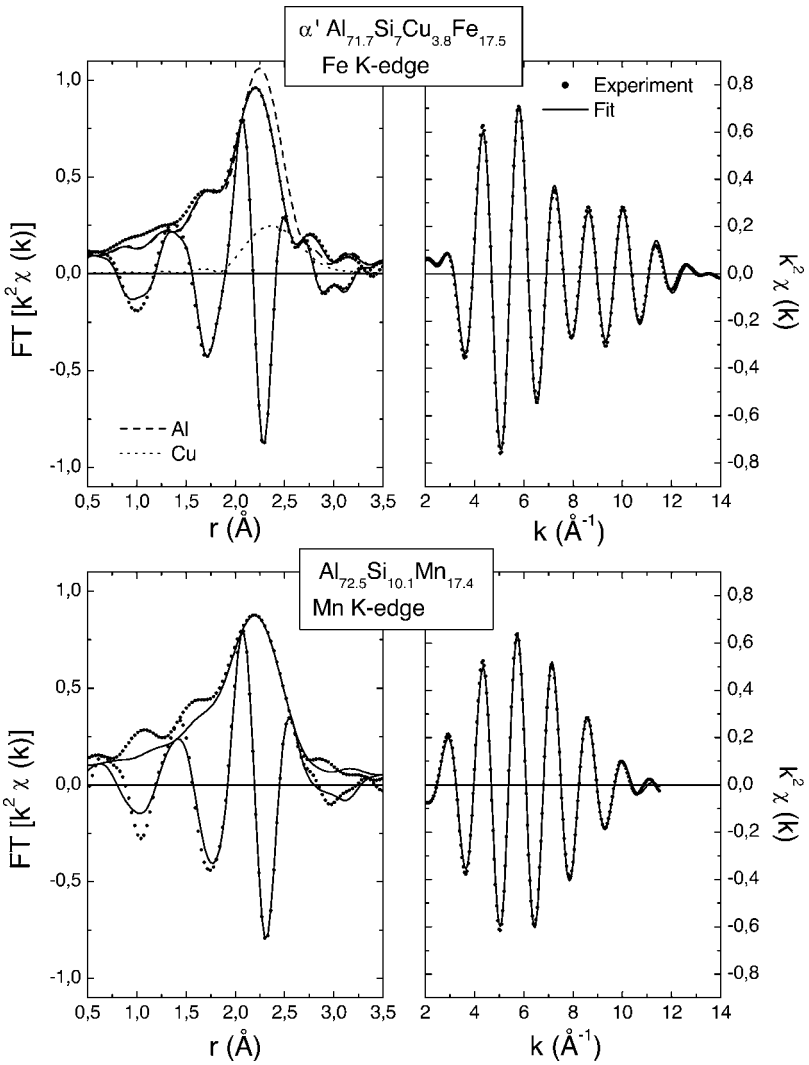

FIG. 3. Amplitude and imaginary part of the FT of $k^2\chi(k)$ (left) and Fourier filtered $k^2\chi(k)$ (right) for α'-$Al_{71.7}Si_7Cu_{3.8}Fe_{17.5}$ at 15 K at the Fe *K*-edge (top) and for $Al_{72.5}Mn_{17.4}Si_{10.1}$ at room temperature at the Mn *K*-edge (bottom). Full circles represent experimental data and solid lines represent the best fits. For α'-Al(Si)-Cu-Fe, the calculated amplitudes of the FT of the Al contribution (dashed line) and of the Cu one (dotted line) are also shown.

A good fit of the experimental FT and IFT at the Mn *K*-edge for the $Al_{72.5}Mn_{17.4}Si_{10.1}$ sample can be obtained by using the structural model of Ref. 26 with $a=12.64$ Å (Table I). All possible single scattering paths corresponding to first neighbors in the distance range [2.3–3.1 Å] around the Mn atoms on sites (5) and (9) were considered. In this distance range, the Mn atoms have only Al(Si) neighbors. The total number of paths amounts to 17. In the fitting procedure, a relative distance change with respect to the initial model ($\delta r/r$) was authorized but assumed to be the same for all paths. It has been found possible to take identical σ^2 values for all individual scattering paths. The parameters resulting from the best fit are presented in Table II where only the total number of Al(Si) neighbors and their average distance from the absorbing Mn atom are given. The only evolution from the starting structural model is a very slight distance reduction. The calculated FT and IFT account well for the experimental data (Fig. 3), except for the FT at very small *r* values where spurious oscillations due to errors in subtracting the absorption background affect the data.

EXAFS oscillations in the α'-$Al_{71.7}Si_7Cu_{3.8}Fe_{17.5}$ phase at the Fe *K*-edge were fitted in a similar way, with $a=12.556$ Å determined from x-ray powder diffraction. An assumption had to be made on the crystallographic sites occupied by the 3.8 at % Cu atoms. Calculations with either no Cu atoms first neighbors of the Fe atoms, or with a random distribution of the Cu atoms on all Al(Si) sites, cannot account for the experimental data. Then we tried to place the Cu atoms on particular Al(Si) sites. The best fits (Fig. 3) are obtained with Cu on the icosidodecahedral shell of the Mackay icosahedra, i.e., on sites (3),(4) and on sites (7),(8) (Table I), which are equivalent due to the body centered symmetry. The obtained parameters are presented in Table II. In order to simplify the presentation of the results, the neighbors have been grouped in "pseudoshells" and only the mean distance of the grouped atoms from the absorbing Fe atom is given. The σ^2 value of an individual scattering path is smaller than in the case of the Al(Si)-Mn phase, in agreement with the difference in measurement temperatures. Contrary to the case of Mn-Al(Si) paths, the σ^2 values of all the individual Fe-Al(Si) paths are not equal. Larger values are found for paths associated with Al(Si) atoms on sites (3),(4),(7),(8), belonging to the icosidodecahedra. Therefore these atoms have been grouped in a separate Al(Si) pseudoshell in Table II. The calculated amplitude of the FT due to all the Cu neighbors and that due to all the Al neighbors are also plotted in Fig. 3. The Cu contribution is out of phase with the Al one, which leads to a decrease of the total am-

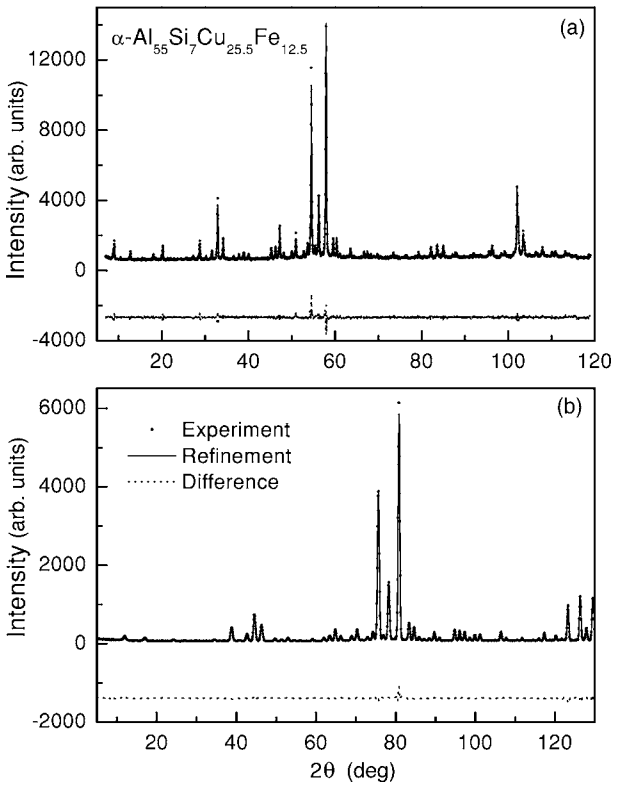

FIG. 4. Rietveld analysis of powder x-ray (a) ($\lambda=1.94$ Å) and neutron (b) ($\lambda=2.593$ Å) diffraction patterns at room temperature: experiment (circles), refinement corresponding to model *A* of Table III (solid line). The difference between the calculated and measured intensities is plotted with an arbitrary vertical shift (dotted line).

plitude with respect to that calculated for Al neighbors only.

In conclusion, these results, in addition to providing a good test of the EXAFS analysis procedure in a complex phase, allowed us to propose Al(Si) substitution sites for the Cu atoms in α'-Al(Si)-Cu-Fe. The obtained solution is close, although not identical, to the one of Ref. 32.

B. α-Al(Si)-Cu-Fe approximant

1. X-ray and neutron powder diffraction for α-$Al_{55}Si_7Cu_{25.5}Fe_{12.5}$

Due to the inability of the structural models of Refs. 23 and 24 to account for the present EXAFS data for α-$Al_{55}Si_7Cu_{25.5}Fe_{12.5}$ (α_1 sample), a new structural determination has been attempted using neutron and x-ray powder diffraction. The neutron coherent scattering lengths are 3.449 fm for Al, 4.1507 for Si, 7.718 for Cu, and 9.45 for Fe, i.e., yielding a significant Fe/Cu contrast, contrary to the case of x-ray scattering.

Experimental data are shown in Fig. 4. X-ray and neutron powder diffraction data were refined simultaneously. For both neutron and x-ray scattering, the Al/Si contrast is small. Indeed attempts to identify particular Si sites were unsuccessful. Hence, Si atoms are treated as Al atoms in the following. The *P* model (Ref. 24) was used as a starting point, the atomic coordinates and the chemical occupations of all crystallographic sites being allowed to vary. The Debye-Waller factors could not be independently fitted due to the insufficient angular range of measurements. They were thus set equal for all sites, except for that of site (2), which was let free to vary independently (Table III).

The calculated structure has 137.1 atoms per unit cell and a cell parameter of 12.329 Å. The refined composition is $Al(Si)_{62.6}Cu_{25.1}Fe_{12.3}$, which is very close to the nominal one. The coordinates of the occupied crystallographic sites are the same as in models *P* and *T*. Several models, with slightly different chemical occupations, were found to give a similar agreement with the data. The reliability factors of these different solutions are, for the x-ray and neutron pattern refinements respectively, rf-factor=7.5 and 4.7 (taking into ac-

TABLE III. Refined structural parameters from Rietveld analysis of x-ray and neutron powder diffraction data for α-$Al_{55}Si_7Cu_{25.5}Fe_{12.5}$ (model A). The isotropic displacement parameter B_{iso} was set to be identical for all sites, except for site (2), and found to be equal to 0.65(5) Å^2. For site (2), an anomalous value [$B_{iso}=27.6(1.0)$ Å^2] is found, revealing a strong disorder.

Atom	No.	Wyckoff	*x*	*y*	*z*	Occupancy
Fe	(1)	1a	0	0	0	1
Al	(2)	12j	0	0.1673(31)	0.1017(35)	0.844(08)
Cu/Al	(3)	24l	0.1166(03)	0.1826(04)	0.2975(03)	0.696(05)/0.304(05)
Cu/Al	(4)	6e	0.3753(07)	0	0	0.619(04)/0.381(04)
Cu/Al/Fe	(5)	12j	0	0.3238(04)	0.1997(05)	0.473(18)/0.205(16)/0.322(16)
Al/Cu	(6)	12k	1/2	0.3322(07)	0.3990(08)	0.774(06)/0.226(06)
Al	(7)	24l	0.3839(05)	0.3114(07)	0.1927(06)	1
Al	(8)	6h	0.1162(12)	1/2	1/2	1
Fe	(9)	12k	1/2	0.1788(03)	0.3018(04)	1
Cu/Al	(10)	6f	0.3135(06)	0	1/2	0.924(09)/0.076(09)
Al	(11)	12j	0	0.3160(09)	0.4066(09)	1
Al	(12)	12k	1/2	0.1290(09)	0.1086(10)	1

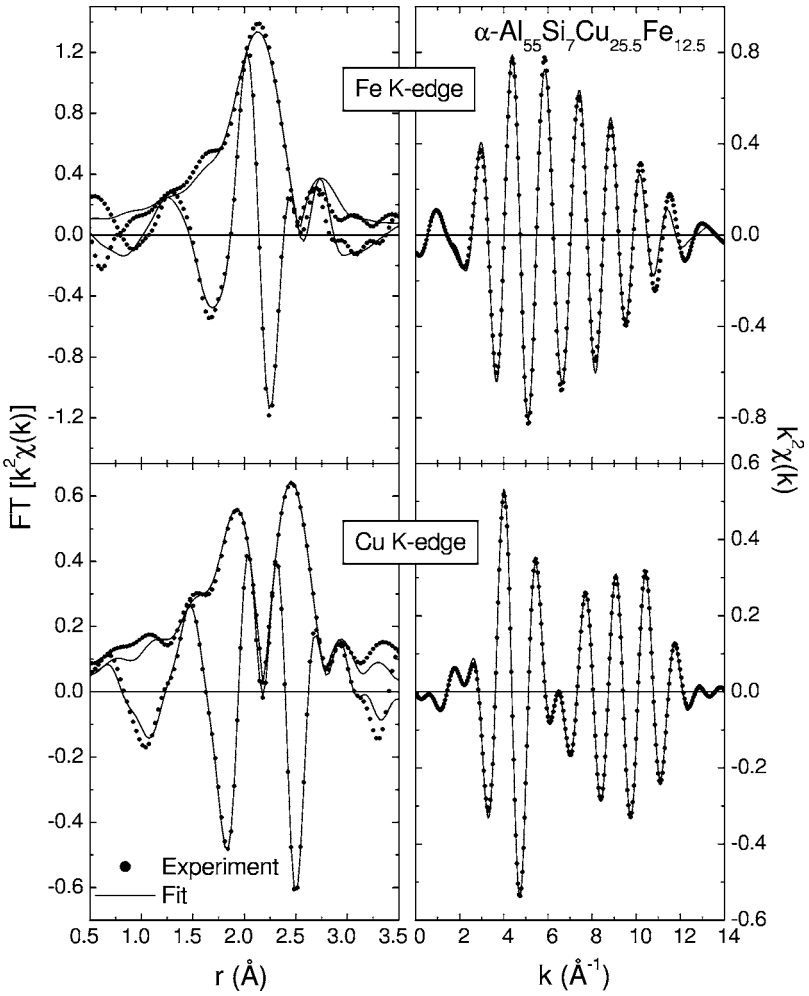

FIG. 5. Amplitude and imaginary part of the FT of $k^2\chi(k)$ (left) and Fourier filtered $k^2\chi(k)$ (right) for α-$Al_{55}Si_7Cu_{25.5}Fe_{12.5}$ at 15 K at the Fe *K*-edge (top) and Cu *K*-edge (bottom). Full circles represent experimental data and solid lines represent the best fits.

count all pattern points) and Bragg *R*-factor=6.5 and 5.2 (taking into account only the pattern points corresponding to Bragg peaks). Note that these values are a bit larger than is usually the case, mainly because of the highly constrained fits resulting from the combined analysis of two different sets of measurements.

For all solutions, sites (2), (7), (8), (11), and (12) are only occupied by Al(Si) atoms. Site (2) is partially occupied by about 10 Al atoms with a large Debye-Waller factor (see Sec. V). Site (1) (origin), as well as site (9) [outer icosahedron of the Mackay cluster at $(1/2,1/2,1/2)$], are occupied by Fe atoms only. The Cu atoms are on sites (3), (4), (5), (6), and (10), all with a chemical disorder. The variations between the different solutions concern the Cu/Al ratio on sites (3), (4), and (6) and the chemical occupation of sites (5) and (10) either by Cu/Al, Cu/Al/Fe or Cu/Fe mixtures. One of the best solutions, denoted as *A* hereafter, is reported in Table III and the corresponding calculated diffracted intensities are given in Fig. 4. In model *A*, sites (5) and (10) are occupied by a mixture of Cu/Al/Fe and Cu/Al atoms respectively. The chemical occupation of the icosahedral clusters in this model is given in Table I.

2. EXAFS results for α-$Al_{55}Si_7Cu_{25.5}Fe_{12.5}$

The experimental EXAFS spectra at the Fe and Cu *K*-edges are presented in Fig. 5. At the Fe *K*-edge, the FT of $k^2\chi(k)$ resembles that of the α'-Al(Si)-Cu-Fe phase, with one main peak exhibiting a small bump on its right-hand side, while the Fourier filtered $k^2\chi(k)$, with a maximum amplitude at *k* values around 5 $Å^{-1}$, is characteristic of an environment where Al(Si) atoms are the majority species. The FT at the Cu *K*-edge is very different, exhibiting two peaks of comparable height.

At each edge, calculations of the EXAFS oscillations were achieved by summing the weighted contributions of the environments of all absorbers on distinct crystallographic sites, as determined from the structural models derived from diffraction data. The fitted *r*-ranges of the FT correspond to first neighbors in the range [2.2–3 Å] around Fe and [2.1–3.15 Å] around Cu. Both Cu and Fe *K*-edges spectra were fitted together. The Si atoms are treated as Al atoms. All the structural models being built on the same atomic structure, the geometry of the possible single scattering paths is model-independent. However, the distribution of the absorbers on distinct crystallographic sites and the nature of the backscattering atoms depends on the chemical decoration and hence on the model. Due to the complexity of atomic environments in the α phase (more than 50 single scattering paths for the Cu absorber for instance) a simplified procedure had to be used to limit the number of fitting variables. The pair distances were allowed to vary but the relative variation with respect to the initial model ($\delta r/r$) was hold identical for

TABLE IV. Structural parameters from the EXAFS fits for the three α-Al(Si)-Cu-Fe samples at the Fe and Cu K-edges. The parameters have been defined in the caption of Table II.

Sample	K-edge	rf	N_{Al}	$\langle r_{Al}\rangle$	$(\delta r/r)_{Al}$	σ^2_{Al}	N_{Cu}	$\langle r_{Cu}\rangle$	$(\delta r/r)_{Cu}$	σ^2_{Cu}	N_{Fe}	$\langle r_{Fe}\rangle$	$(\delta r/r)_{Fe}$	σ^2_{Fe}
α_1	Fe	0.016	9.06	2.588	0.0116	0.0039	2.09	2.702	−0.0066	0.0039				
	Cu	0.002	7.63	2.645	−0.0082	0.0048	3.32	2.725	0.0042	0.0048	1.03	2.702	−0.0066	0.0039
α_2	Fe	0.007	9.31	2.625	0.0173	0.0018	1.93	2.655	−0.0041	0.0018				
	Cu	0.003	8.68	2.644	−0.0096	0.0037	1.78	2.872	0.0123	0.0037	1.56	2.655	−0.0041	0.0018
α_3	Fe	0.011	9.32	2.574	0.0115	0.0048	1.74	2.732	−0.0171	0.0048				
	Cu	0.003	7.62	2.639	−0.0113	0.0040	3.27	2.692	0.0018	0.0040	0.86	2.732	−0.0171	0.0048

a given kind of pair (given chemical nature of the absorbing and backscattering atoms). Due to the simultaneous fit of both the Fe and Cu K-edges EXAFS oscillations, a common set of refined Cu-Fe distances is automatically obtained. For a given absorber, the same σ^2 value was imposed for all scattering paths involving a backscattering atom of the same chemical nature. In addition, the σ^2 value for a Fe atom around an absorbing Cu atom was held equal to that for a Cu atom around a Fe absorbing atom.

The EXAFS calculations were performed in two steps. First, the chemical occupation given by the different structural models was kept fixed. Then, for each model, the experimental FT and IFT at the Fe and Cu K-edges were fitted with varying distances ($\delta r/r$), σ^2 values and energy shifts (ΔE_0). The P model was found unable to account for the EXAFS spectra either at the Cu or at the Fe K-edges. Calculations obtained by starting from the T model are slightly closer to the experimental data, but still not satisfactory. Better results were obtained starting from the different models obtained from the analysis of the present x-ray and neutron diffraction patterns (Sec. IV B 1). Then, in a second step, the investigations were restricted to this class of models. Let us recall that they differ only by the chemical occupation of crystallographic sites (3), (4), (5), (6), and (10). Therefore, in the EXAFS fits, the chemical nature of the atoms on these sites was allowed to vary, with the total Cu, Al and Fe concentrations held constant and equal to the nominal ones. For the other crystallographic sites, occupied by a single chemical species [Fe on sites (1) and (9) and Al on sites (2), (7), (8), (11), and (12)], no changes were allowed. It must be emphasized that a simultaneous fit of the Fe and Cu K-edges is essential in order to extract a coherent model of the chemical occupations.

The structural parameters deduced from the best fit of the EXAFS oscillations, obtained by starting from model A, are listed in Table IV and the refined chemical decoration (model B) is presented in Table I. As for the case of the α' phase, a pseudoshell description is used in Table IV, in order to simplify the presentation of the results. Here all neighbors of a given chemical nature have been grouped together in the same pseudoshell. The best fits of the FT and IFT are shown in Fig. 5. Considering the great complexity of the atomic environment in this sample and to the highly constrained type of fit, the results can be considered as satisfactory. The refined chemical decoration differs only slightly from the initial one (model A).[37] In the final model B, sites (4) and (10) are occupied by Cu atoms only, instead of an Al/Cu mixture in the initial model and a larger proportion of Al atoms is found in site (3). The Fe atoms are found to occupy completely sites (1) and (9) like in the initial model, and partially site (5). Therefore, in the final model, the only sites with a mixed occupation are (3) and (6) with a Cu/Al mixture and (5) with a Cu/Al/Fe mixture. Note that the transfer of a small amount of Fe from site (5) to site (10) is possible but does not improve the fit.

The decomposition of the FT and IFT of the refined model for each kind of neighbor (Al, Cu or Fe) around a given absorber (Figs. 6 and 7) allows one to understand the overall shapes of the FT and IFT. It should be emphasized that the Fe atoms have no Fe first neighbors. At the Cu K-edge, the double peak shape and the sharp dip in the FT at 2.4 Å are demonstrated to come mainly from destructive interference between the Al and Cu contributions, the imaginary parts of the FT having opposite phases.

3. Evolution of the chemical order with composition

EXAFS results for two additional samples $Al_{60.5}Si_7Cu_{18}Fe_{14.5}$ (α_2) and $Al_{57}Si_5Cu_{27}Fe_{11}$ (α_3) will be discussed in this section where the evolution of the chemical order with composition will be addressed. From the existence domain of α-Al(Si)-Cu-Fe (Fig. 1), the lowest possible Fe concentration is 9.8 at %, which corresponds to about 13 Fe atoms per unit cell. In the case of α_1, the previous results (Table I) lead to 13 Fe atoms completely occupying sites (1) (origin) and (9) [outer icosahedron of the Mackay cluster at (1/2,1/2,1/2)] while 4 other Fe atoms partially occupy site (5) [outer icosahedron of the Mackay cluster at (0, 0, 0)]. From these results, it is reasonable to assume: (i) a complete occupation of sites (1) and (9) by Fe atoms in all α phases whatever their composition, (ii) a progressive introduction of Fe on site (5) when the Fe composition increases from 9.8 to 15.2 at % throughout the existence domain of the α phase. Then, for the maximum possible Fe concentration, site (5) would be occupied by 7.7 Fe atoms. The variations of the Cu concentration within the existence domain of α (from 16.5 up to 28.5 at %) can be explained by variations of the chemical occupation of one, or several, of the sites with a possible mixed occupation [Al/Cu for sites (3), (4), (6), and (10) and Al/Cu/Fe for site (5)].

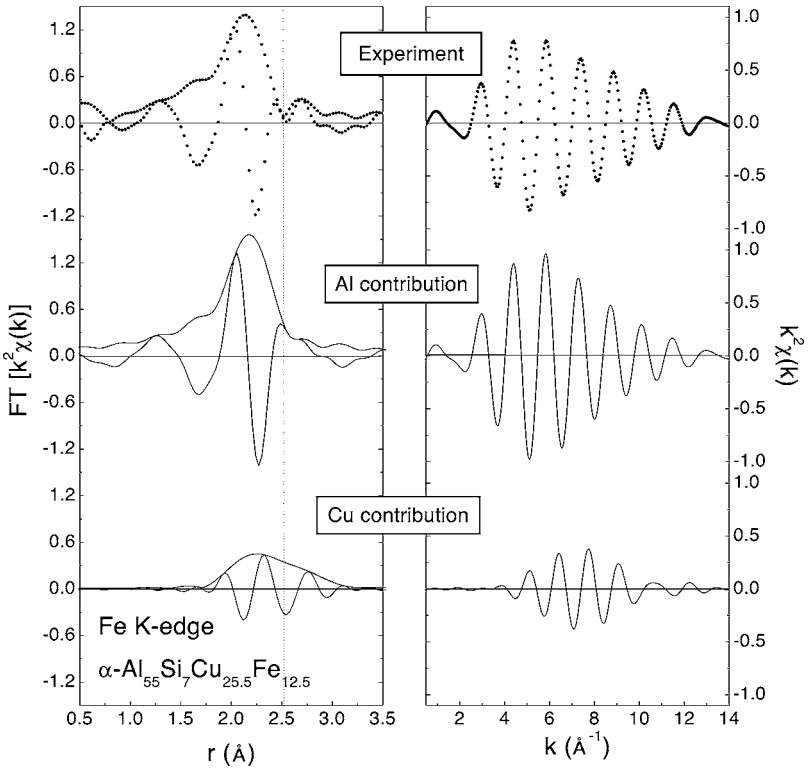

FIG. 6. Amplitude and imaginary part of the FT of $k^2\chi(k)$ (left) and Fourier filtered $k^2\chi(k)$ (right) for α-$Al_{55}Si_7Cu_{25.5}Fe_{12.5}$ at 15 K at the Fe *K*-edge. From top to bottom: experimental data, results of the best fits for the Al and Cu contributions. The vertical line indicates the *r* value at which the Cu and Al contributions to the FT have opposite phases, yielding destructive interference in the total FT.

Having in mind these possible trends, the substitution mechanisms can now be analyzed through the study of the EXAFS oscillations at the Fe and Cu *K*-edges measured for α_2 and α_3 samples. The composition changes from α_1 to α_2 correspond to an addition of 2.7 Fe and 7.5 Al and the suppression of 10.2 Cu per unit cell. For α_3, there are 2 Fe atoms less and 2 Cu more than for α_1, the total Al(Si) content remaining unchanged but the Si composition decreasing from 7 to 5 at %. As shown in Fig. 8, the measured FTs at the Fe *K*-edge vary very little with composition. In contrast, the composition dependence of the FT is much stronger at the Cu *K*-edge: the relative height of the two peaks varies significantly with the composition. This evolution is partly due to the sensitivity of the interference dip to small structural changes.

The structural model, used as a starting point to fit EXAFS oscillations for α_2 and α_3, is model A of Table III, with slightly modified chemical decorations in order to match the sample composition. In the fitting procedure, the Fe content was allowed to vary only on site (5), the Al/Cu chemical occupation of sites (3), (4), (5), (6), and (10) was let free, with the total Cu, Al, and Fe concentrations held constant and equal to the nominal one.

The resulting fits (Fig. 8) agree well with the experimental spectra for both α_2 and α_3 samples, especially at the Cu *K*-edge where the variation of the double peak with composition is accounted for. The obtained structural parameters are listed in Table IV, using a pseudoshell description, and the refined chemical decoration is presented in Table I. There are slight pair distance and σ^2 value variations with respect to α_1 but the most important changes concern the chemical decoration. The Cu atoms occupying site (5) in α_1 are totally replaced by 2.7 Fe and 2.3 Al atoms in the α_2 sample. In addition, about 4.6 Cu atoms in sites (3) and (6) in α_1 sample are changed into Al in α_2. When comparing α_3 and α_1, the only significant change is the replacement in site (5) of 2 Fe (in α_1) by 2 Cu atoms (in α_3), the remaining chemical decoration being very similar for both samples. Therefore, the modification of Si concentration from 7 to 5 at %, holding constant the total Al/Si content, does not induce a significant chemical decoration rearrangement. In conclusion, the EXAFS results suggest rather simple substitution rules for the studied samples. The changes in Fe and related Cu concentration occur through varying the occupation on site (5), while additional variations of the Cu/Al content may occur on sites (5), (3), and (6).

V. DISCUSSION

A. Structure and stability of 1/1 approximants

In this section, the present results for the atomic structure of α' and α-Al(Si)-Cu-Fe phases will be compared with that of other 1/1 approximants of quasicrystals. Similar cubic structures, based on Mackay clusters have been found in 1/1 approximants in the Al(Si)-Re,[30] Al-Cu-Ru,[31] and Al(Si)-Cu-Ru (Ref. 32) systems. On the contrary, quite different atomic structures, based on Bergman clusters have been found in Al-Li-Cu and Al-Mg-Zn approximants,[11,38,39] while the 1/1 Al(Si)-Pd-Mn approximant exhibits a particular structure.[40,41]

Among cubic approximants with Mackay clusters, the 1/1 Al(Si)-Mn, Al(Si)-Re, and α'-Al(Si)-Cu-Fe phases are isomorphous, neglecting the primitive or body center character.[29] The existence of a similar phase has been reported in the Al(Si)-(Fe,Ru)-Cu system, with the Ru atoms

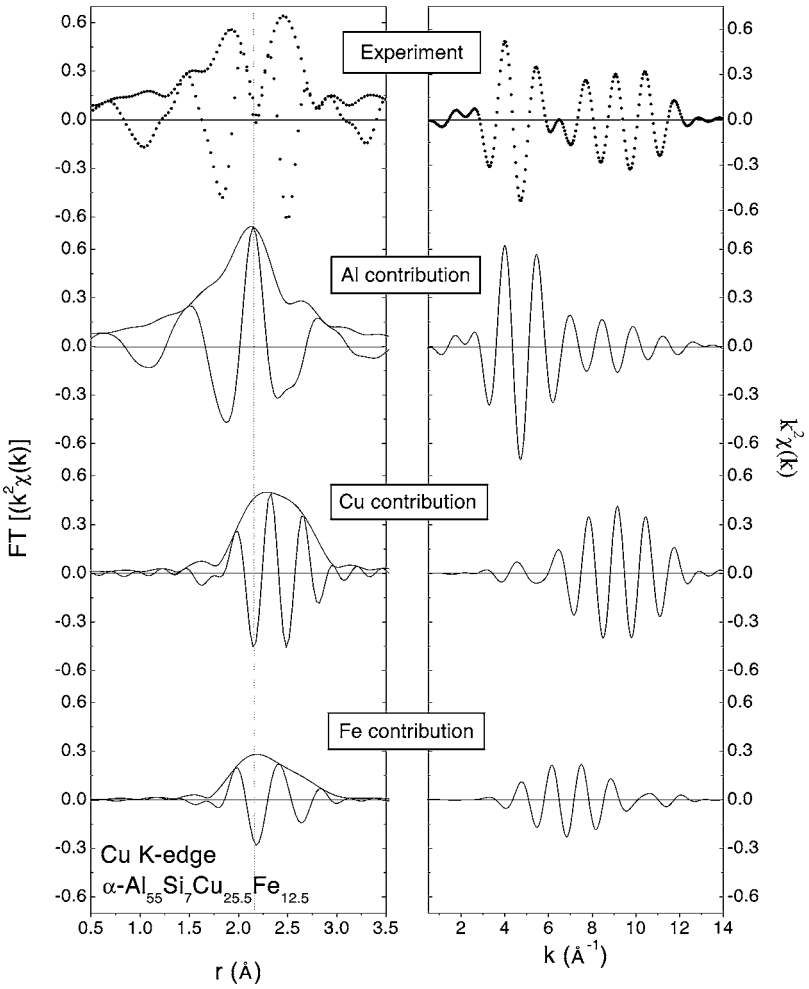

FIG. 7. Amplitude and imaginary part of the FT of $k^2\chi(k)$ (left) and Fourier filtered $k^2\chi(k)$ (right) for α-$Al_{55}Si_7Cu_{25.5}Fe_{12.5}$ at 15 K at the Cu K-edge. From top to bottom: experimental data, results of the best fits for the Al, Cu, and Fe contributions. The vertical line indicates the r value at which the Cu and Al contributions to the FT have opposite phases, yielding destructive interference in the total FT.

replacing the Fe ones in the α' phase.[32] In all these phases, the transition atoms (Re, Mn or Fe) fully occupy the two outer icosahedra of the Mackay clusters [sites labeled (5) and (9) in the present work]. The Mackay clusters centered at (0,0,0) and $(1/2,1/2,1/2)$ are identical and their centers are empty. On the contrary, in the α-Al(Si)-Cu-Fe, the two Mackay clusters do not have the same chemical decoration. Nevertheless, it is striking to note that, in the three studied α-Al(Si)-Cu-Fe samples, Fe atoms are found on the outer icosahedra of the two Mackay clusters, fully occupying site (9) and partly site (5). In addition, the (0,0,0) position is occupied by a Fe atom, the $(1/2,1/2,1/2)$ one remaining empty. It is interesting to compare these results with the atomic structure of the $Al_{57.3}Cu_{31.4}Ru_{11.3}$ which has been identified as a 1/1 approximant in the Al-Cu-Ru system (without Si).[31] The Ru composition corresponds to 14 Ru per unit cell occupying the outer icosahedron of the Mackay cluster at $(1/2,1/2,1/2)$ [site (9)] and the two centers of the Mackay clusters (see Table I). The presence of a central atom has a strong influence on its first neighbors. When the center of the cluster is vacant, the first shell is a perfect icosahedron, as drawn in Fig. 2. This is no longer the case if the center is occupied. It is still possible to fit diffraction data by introducing a partial occupancy of the crystallographic position [site (2) for the Mackay centered at the origin or (6) for the Mackay centered at $(1/2,1/2,1/2)$] but an abnormally large Debye-Waller factor is then obtained, indicating strong displacements from the icosahedral positions (Table III). This structural relaxation within the first shell has been described as a phasonlike phenomenon in Ref. 24. In Ref. 23, Takeuchi *et al.* proposed to replace site (2) by three distinct crystallographic sites with low occupations. In Ref. 31, the structure of the first shell is interpreted as an intermediate between icosahedral and rhombic dodecahedral symmetries.

In conclusion, a common feature of all the 1/1 approximants with Mackay clusters is that the transition atoms occupy the outer icosahedra of the Mackay clusters [sites (5) and (9)]. The only exception seems to be the $Al_{54}Si_8Cu_{25.5}Ru_{12.5}$ phase[32] where 4 Ru atoms occupy partially site (10), while site (5) is occupied by a mixture of Al and Cu, site (9) being occupied by 12 Ru atoms like in the other approximants. This structure corresponds to model T for the α-Al(Si)-Cu-Fe phase,[23] which was found here unable to account for the neutron and EXAFS data. It is interesting to discuss the link between the chemical order and the stability domains of these phases. When the two icosahedra are filled by transition atoms, their total number per unit cell amounts to 24, leading to a transition metal composition equal to 17.4 at %. It is striking to note that these phases [1/1 Al(Si)-Mn, Al(Si)-Re, and α'-Al(Si)-(Cu,Ru)-Fe] only exist for this particular composition and that all efforts to vary the transition metal composition lead to non single-phase samples.[16,30] On the other hand, the 1/1 approximant

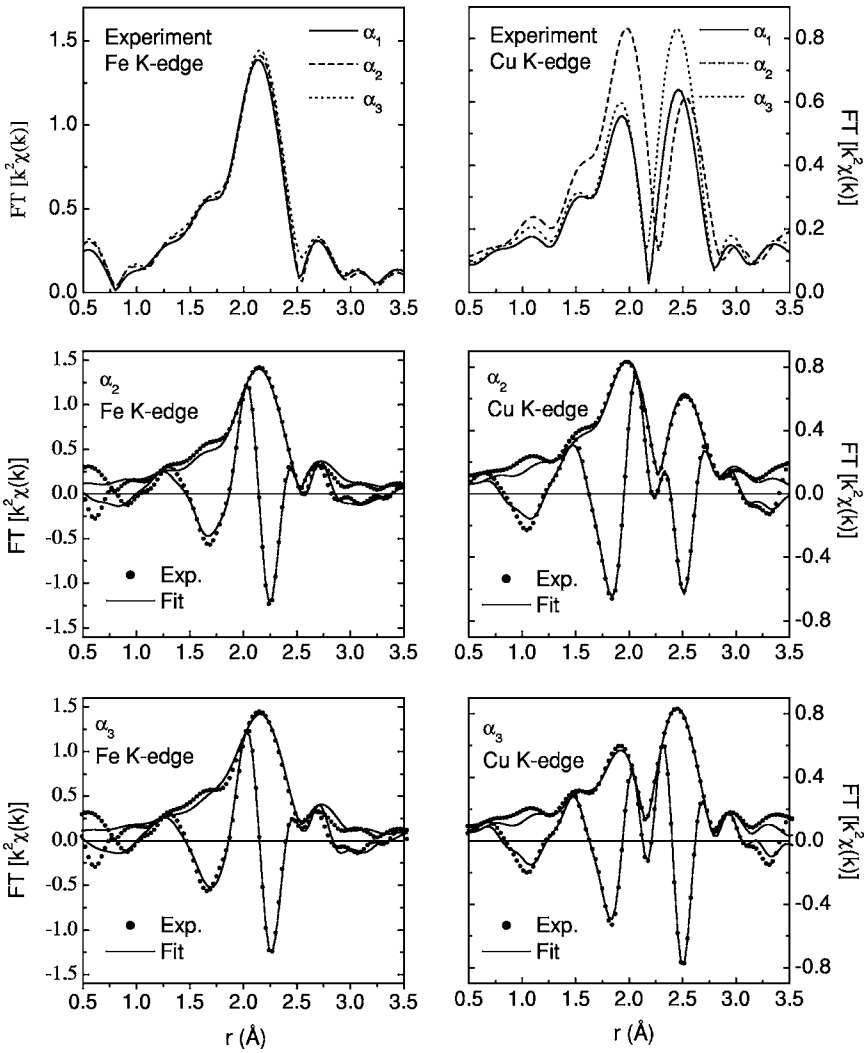

FIG. 8. Experimental amplitude of the FT of $k^2\chi(k)$ at the Fe K-edge (left) and Cu K-edge (right) for the three studied α-Al(Si)-Cu-Fe samples (top). Comparison of the amplitude and imaginary part of the FT for the experimental data (full circles) and for their best fits (solid lines) at the Fe and Cu K-edges for α_2 (middle) and α_3 (bottom).

in the Al-Cu-Ru system has been reported to exist for the $Al_{57.3}Cu_{31.4}Ru_{11.3}$ composition, which corresponds to the filling by Ru atoms of only one icosahedron, on the Mackay cluster at $(1/2,1/2,1/2)$. The outer icosahedron of the Mackay cluster at (0,0,0) contains Al and Cu atoms. Therefore, the case of the α-Al(Si)-Cu-Fe phase which exists in a small composition domain (Fig. 1) is particular. The present results suggest that this existence domain is related to a progressive introduction of Fe atoms on the outer icosahedron of the Mackay cluster centered at (0,0,0), starting from 0 Fe atoms for a nominal Fe content of 9.8 at % to 7.7 Fe atoms for a nominal Fe content of 15.2 at %. In addition, the fact that site (5) would be occupied by a mixture of Al(Si), Cu and Fe atoms provides an explanation for the substitution law determining the elongated shape of the existence domain (1 Cu being replaced by 0.6 Al+0.4 Fe).

However, from these structural considerations only, one cannot explain why the maximum Fe concentration is 15.2 at % α-Al(Si)-Cu-Fe phase, or, stated in a different way, why the filling of the outer icosahedron of the Mackay cluster at $(1/2,1/2,1/2)$ by Fe atoms is limited to 7.7 Fe atoms. This is all the more surprising as the complete filling of this icosahedron is indeed observed in the α'-Al(Si)-Cu-Fe phase. An answer to this question is required to explain the coexistence of two distinct cubic Al(Si)-Cu-Fe phases, with the same atomic structure, but within separate composition domains. It would involve considerations on stability criteria, which are beyond the scope of the present work. However, it is interesting to recall that for approximants, as well as for quasicrystals, a stability of electronic origin, closely linked with the formation of a pseudogap in the density of states at the Fermi level, has often been invoked. This mechanism is related to the Hume-Rothery picture of phase stability. Indeed, the elongated shape of the existence domains of the QC or α phases corresponds to a constant average number of conduction electrons per atom (e/a). In a rough Hume-Rothery like argument, one obtains $e/a=1.865$ for the QC phases and $e/a=1.935$ for the α_1 phase, assuming valences equal to +3 for Al, +4 for Si, +1 for Cu, and −2 for Fe. The small difference between these two e/a values results only from the substitution of a few at % of Al by Si atoms in the α phase. For the α', one finds $e/a=2.10$. In view of the closeness of these two e/a values, it is mandatory to go further than the use of such rough arguments. This requires electronic band calculations of realistic structures, with the correct chemical decoration, which would actually be possible for the two 1/1 approximants by using the structures determined in the present work.

Another way to analyze the chemical decoration is to describe the local environment around the transition metal atoms. A striking feature is that, in all these 1/1 approximants, the transition metal atoms are never first neighbors. In the α-Al(Si)-Cu-Fe phase, among the 11.2 neighbors constituting the average environment of Fe atoms, one finds between 9.1 and 9.3 Al(Si) atoms, and about 2 Cu atoms, for the three studied samples, which span the concentration existence domain of the phase (Table IV). The number of Cu atoms first neighbors of Fe atoms is smaller than 3.1, expected value if Al, Cu, and Fe atoms had been distributed randomly on the atomic sites. These observations point out a strong chemical affinity between Al and Fe atoms and more generally between Al and transition metal atoms. A similar observation has been drawn from the study of Al-Co-Fe liquids[42] and Al-Mn liquids in equilibrium with QCs or approximants.[43]

B. Interest of EXAFS studies

The central role of EXAFS studies in the present work has to be emphasized. First, the EXAFS sensitivity to chemical order allowed us to demonstrate that the previously published structural models did not provide a correct description of the α-Al(Si)-Cu-Fe structure. This observation was indeed the reason that led us to perform new diffraction experiments. Secondly, although the combination of neutron and x-ray scattering allowed us to improve the structural model, ambiguities remained, which could be removed by the EXAFS analysis. Finally the sensitivity of EXAFS oscillation to minor changes in the chemical order, especially around Cu, allowed us to understand the chemical substitution law underlying the existence domain of α-Al(Si)-Cu-Fe. However, in the case of phases with a large unit cell and chemical disorder, as it is indeed the case for the α-Al(Si)-Cu-Fe 1/1 approximant, the EXAFS treatment is complicated. One has to consider the local environment for each of the crystallographic sites occupied by the absorbing atom and then to sum the EXAFS oscillations given by Eq. (1) over all possible scattering paths. Such a summation is complex, even when limited to first neighbors. More than 50 single scattering paths are necessary to describe EXAFS oscillations at the Cu K-edge in the α phase. Besides, one has to adjust the chemical occupancy of all sites in a self-coherent way. One has to emphasize that such an analysis of the EXAFS oscillations is mandatory and that a simplified treatment, although often used in the literature, leads to erroneous conclusions. The simplified EXAFS analysis consists in grouping neighbors of the same nature in atomic shells with a Gaussian distance distribution around an averaged distance. Then the averaged distance and the total number of atoms within the shell are introduced in Eq. (1), the distance distribution within the shell being accounted for by the σ^2 value. In the case of the α-Al(Si)-Cu-Fe 1/1 approximant, we have found that such a method is misleading. Destructive interferences occur between the individual paths and the summed contributions of all Al, Cu or Fe neighbors are non-Gaussian. This is especially clear for the Cu K-edge spectrum presented in Fig. 7.

VI. CONCLUSION AND PERSPECTIVES

In the present work, the structure and especially the chemical decoration of 1/1 approximants in the Al(Si)-Cu-Fe system was determined by using joined refinements of x-ray and neutron diffraction data and thorough EXAFS analysis. The structure of the α phase is shown to accommodate a great chemical disorder with mixed sites involving two (Cu/Al) and even three (Cu/Al/Fe) different chemical species, in addition to sites occupied only by Fe or Al(Si) atoms. These original results allow one to understand the composition variations in the phase diagram within an elongated existence domain for the α phase. In spite of this high disorder, the Fe atoms are found on the outer icosahedron of the two Mackay clusters centered at (0, 0, 0) and $(1/2,1/2,1/2)$. The same feature is observed in the α'-Al(Si)Cu-Fe phase and for Mn and Ru atoms in 1/1 Al(Si)-Mn and Al-Cu-Ru approximants respectively. Such a precise determination of the atomic structure of approximants is a necessary step for electronic band structure calculations, required to understand the electronic properties and the stability of approximants and QC. These calculations should then help to resolve a puzzling point, i.e., the existence of two 1/1 approximants in the Al(Si)-Cu-Fe system with the same atomic structure in distinct existence composition domains.

The determination of the chemical decoration in approximants is also very important in order to get an insight into that in the quasicrystal. The theoretical model of the F-type icosahedral phases in 6D representation[6] can be used to generate the quasiperiodic structure in 3D with, however, remaining uncertainties in the chemical decoration. In the present case, the composition of α-$Al_{55}Si_7Cu_{25.5}Fe_{12.5}$ phase is very close to that of the $Al_{62}Cu_{25.5}Fe_{12.5}$ quasicrystal. The EXAFS spectra in the QC phase[44] are indeed very similar to the ones measured for the α phase. Therefore, the presently determined structure of the α phase should be a good starting point for the structure determination of the QC one using the type of EXAFS analysis presented in this work, i.e., beyond the usual model based on few Gaussian shells and leading to unrealistic low coordination numbers.[44]

ACKNOWLEDGMENTS

We would like to thank M. Audier (LMGP) and A. Traverse (LURE) for fruitful discussions. We are grateful to B. Bochu (LMGP), for his assistance for the x-ray powder diffraction measurement, and to R. Bellissent (LLB), for the neutron powder diffraction experiment. We also thank F. Puyraimond, M. Quiquandon, and D. Gratias (LEM, CNRS/ONERA) for very interesting discussions about their structural model prior to its publication.

*Electronic address: Virginie.Simonet@grenoble.cnrs.fr

[1] A. P. Tsai, A. Inoue, and T. Masumoto, Jpn. J. Appl. Phys., Part 1 **26**, L1505 (1987); **27**, 1587 (1988); A. P. Tsai, A. Inoue, Y. Yokoyama, and T. Masumoto, Philos. Mag. Lett. **61**, 9 (1990); A. P. Tsai, Y. Yokoyama, A. Inoue, and T. Masumoto, Jpn. J. Appl. Phys., Part 1 **29**, 1161 (1990).

[2] *Physical Properties of Quasicrystals*, edited by Z. M. Stadnik (Springer, Berlin, 1999).

[3] E. Belin-Ferré, J. Phys.: Condens. Matter **14**, R789 (2002).

[4] M. Duneau and A. Katz, Phys. Rev. Lett. **54**, 2688 (1985).

[5] V. Elser, Acta Crystallogr., Sect. A: Found. Crystallogr. **42**, 36 (1986).

[6] D. Gratias, F. Puyraimond, M. Quiquandon, and A. Katz, Phys. Rev. B **63**, 024202 (2000).

[7] A. Yamamoto, H. Takakura, and A. P. Tsai, Phys. Rev. B **68**, 094201 (2003).

[8] G. Trambly de Laissardière, D. Mayou, and D. Nguyen Manh, Europhys. Lett. **21**, 25 (1993); G. Trambly de Laissardière, D. Nguyen Manh, L. Magaud, J. P. Julien, F. Cyrot-Lackmann, and D. Mayou, Phys. Rev. B **52**, 7920 (1995).

[9] A. L. Mackay, Acta Crystallogr. **15**, 916 (1962).

[10] G. Bergman, J. L. T. Waugh, and L. Pauling L, Acta Crystallogr. **10**, 254 (1957).

[11] U. Mizutani, T. Takeuchi, and H. Sato, J. Phys.: Condens. Matter **14**, R767 (2002).

[12] R. A. Brand, J. Pelloth, F. Hippert, and Y. Calvayrac, J. Phys.: Condens. Matter **11**, 7523 (1999). F. Hippert, R. A. Brand, J. Pelloth, and Y. Calvayrac, *ibid.* **6**, 11189 (1994).

[13] M. Krajči, M. Windisch, J. Hafner, G. Kresse, and M. Mihalkovič, Phys. Rev. B **51**, 17355 (1995).

[14] G. Trambly de Laissardière and T. Fujiwara, Phys. Rev. B **50**, 5999 (1994).

[15] M. Quiquandon, A. Quivy, J. Devaud, F. Faudot, S. Lefebvre, M. Bessière, and Y. Calvayrac, J. Phys.: Condens. Matter **8**, 2487 (1996).

[16] M. Quiquandon, Y. Calvayrac, A. Quivy, F. Faudot, and D. Gratias, in *Quasicrystals*, MRS Symposia Proc. No. 553 (Materials Research Society, Pittsburgh, 1999), p. 95.

[17] E. Belin, Z. Dankhazi, A. Sadoc, Y. Calvayrac, T. Klein, and J. M. Dubois, J. Phys.: Condens. Matter **4**, 4459 (1992).

[18] D. Mayou, C. Berger, F. Cyrot-Lackmann, T. Klein, and P. Lanco, Phys. Rev. Lett. **70**, 3915 (1993).

[19] A. Quivy, M. Quiquandon, Y. Calvayrac, F. Faudot, D. Gratias, C. Berger, R. A. Brand, V. Simonet, and F. Hippert, J. Phys.: Condens. Matter **8**, 4223 (1996).

[20] The boundaries of the existence domain of α in Fig. 1 differ slightly from those shown in Fig. 8 of Ref. 16 where a drawing error occurred.

[21] M. Cooper, Acta Crystallogr. **23**, 1106 (1967).

[22] T. Takeuchi and U. Mizutani, J. Alloys Compd. **342**, 416 (2002).

[23] T. Takeuchi, H. Yamada, M. Takata, T. Nakata, N. Tanaka, and U. Mizutani, in *Proceedings of the 7th International Conference on Quasicrystals*, Stuttgart, 1999, edited by F. Gähler, P. Kramer, H-R. Trebin, and K. Urban, Science and Eng. A **294–296**, 340 (2000); Z. Stadnik, T. Takeuchi, N. Tanaka, and U. Mizutani, J. Phys.: Condens. Matter **15**, 6365 (2003).

[24] F. Puyraimond, M. Quiquandon, D. Gratias, M. Tillard, C. Belin, A. Quivy, and Y. Calvayrac, Acta Crystallogr., Sect. A: Found. Crystallogr. **58**, 391 (2002).

[25] M. Cooper and K. Robinson, Acta Crystallogr. **20**, 614 (1966).

[26] K. Sugiyama, N. Kaji, and K. Hiraga, Acta Crystallogr., Sect. C: Cryst. Struct. Commun. **54**, 445 (1998).

[27] P. Guyot and M. Audier, Philos. Mag. B **52**, L15 (1985).

[28] V. Elser and C. L. Henley, Phys. Rev. Lett. **55**, 2883 (1985).

[29] According to Cooper in Ref. 21, the body centered character of the α'-Al(Si)-Fe phase results from the coexistence of two different primitive unit cells. In this description, the 1/1 Al(Si) -Mn unit cell is strictly isomorphous to the Al(Si)-Fe cell labeled 1 in Ref. 21.

[30] T. Takeuchi, T. Onogi, S. Otagiri, U. Mizutani, H. Sato, K. Kato, and T. Kamiyama, Phys. Rev. B **68**, 184203 (2003); T. Onogi, T. Takeuchi, H. Sato, and U. Mizutani, J. Alloys Compd. **342**, 397 (2002).

[31] K. Sugiyama, T. Kato, T. Ogawa, K. Hiraga, and K. Saito, J. Alloys Compd. **299**, 169 (2000).

[32] T. Takeuchi and U. Mizutani, J. Alloys Compd. **342**, 416 (2002); U. Mizutani, T. Takeuchi, E. Banno, V. Fournée, M. Takata, and H. Sato, MRS Symposia Proceedings No. 643 (Materials Research Society, Pittsburgh, 2001), K.13.3.1.

[33] J. Rodriguez-Carvajal, Physica B **192**, 55 (1993) and IUCR Commission on Powder Diffraction fraction Newsletter **26**, 12 (2001), available at http://journals.iucr.org/iucr-top/comm/cpd/Newsletters/. The complete program and documentation can be obtained from the anonymous ftp-site: ftp://ftp.cea.fr/pub/llb/divers/fullprof.2k.

[34] M. Newville, P. Livins, Y. Yacoby, J. J. Rehr, and E. A. Stern, Phys. Rev. B **47**, 14126 (1993); S. I. Zabinsky, J. J. Rehr, A. Ankudinov, R. C. Albers, and M. J. Eller, *ibid.* **52**, 2995 (1995); M. Newville, R. Ravel, D. Haskel, J. J. Rehr, E. A. Stern, and Y. Yacoby, Physica B **208–209**, 1547 (1995).

[35] M. G. Bown and P. J. Brown, Acta Crystallogr. **9**, 911 (1956).

[36] In practice, for a given absorber, slightly different shifts of the edge energy ΔE_0 were introduced, one for each kind of neighboring atoms (Al, Cu or Fe). These different E_0 shifts are meant to correct minor errors introduced by FEFF in the calculation of the scattering phase shifts.

[37] Using the atomic positions and the DW factors of the initial model A, we can calculate the x-ray and neutron diffraction patterns expected for the chemical decoration of model *B*, deduced from EXAFS analysis. The calculated patterns account for the experimental diffraction data, with reliability factors close to those obtained for model A.

[38] M. Audier, J. Pannetier, M. Leblanc, C. Janot, J. M. Lang, and B. Dubost, Physica B **153**, 136 (1988).

[39] T. Takeuchi and U. Mizutani, Phys. Rev. B **52**, 9300 (1995).

[40] K. Sugiyama, N. Kaji, and K. Hiraga, Z. Kristallogr. **213**, 168 (1998).

[41] A. Yamamoto and H. Takakura, Phys. Rev. B **68**, 132201 (2003).

[42] T. Schenk, V. Simonet, D. Holland-Moritz, R. Bellissent, T. Hansen, P. Convert, and D. M. Herlach, Europhys. Lett. **65**, 34 (2003).

[43] V. Simonet, F. Hippert, M. Audier, and R. Bellissent, Phys. Rev. B **65**, 024203 (2001).

[44] A. Sadoc, C. Berger, and Y. Calvayrac, Philos. Mag. B **68**, 475 (1993).